Cost-Effectiveness Studies of the BESSs Participating in Frequency Regulation

Tian Zhang
Hoay Beng Gooi
School of Electrical and Electronic Engineering
Nanyang Technological University
Singapore, 639798
Email: tzhang013@e.ntu.edu.sg, ehbgooi@ntu.edu.sg

Shuaixun Chen
Terence Goh
DNV GL Energy (formerly KEMA)
Singapore
Email: nosper@pmail.ntu.edu.sg, Terence.Goh@dnvgl.com

***Abstract*—With the more advanced technology and decreased cost of batteries, it is less costly to form large-scale battery energy storage systems (BESSs) to take part in grid applications. BESSs are increasingly considered as participants for grid regulation services because of their fast responding ability. This paper reviews various control schemes of the BESSs in the literature. Sizing studies are conducted based on the current regulation performance scoring system and the respective criteria, using historical regulation data. The cost and lifetime of three mainstream batteries (Lead-acid, Lithium-ion, and Vanadium) are estimated. Cost-performance indexes are calculated based on simulation results.**

***Index Terms*—Frequency Regulation, Battery Energy Storage System (BESS), cost-performance index.**

I. Control Schemes of BESSs

With the increasing penetration rate of intermittent renewable energy sources (RESs) such as solar and wind power, system frequency regulation requires a larger capacity, as well as a faster responding speed. Battery energy storage systems (BESSs) have been under research to contribute to system frequency control, due to its fast responding ability to follow the fluctuating regulation signal. Furthermore, with the cost reduction of batteries in recent years, grid-scale BESSs are becoming more favorable to participate in the system regulation services.

In early research studies, a proportional frequency error is always directly used as the BESS control signal to study the BESSs' ability to follow the regulation commands [1], [2], [3]. BESSs are proven to be effective in improving system frequency.

However, as a storage device, the battery holds limited amount of energy. More sophisticated control schemes are developed according to the characteristics of the BESSs. There are mainly two categories of control schemes described as follows.

1. SOC-based participation factor modification: The power output of the BESS is compromised according to the SOC information. As long as the system frequency dynamics are within the limit, the BESS commands are modified to absorb more/less energy to maintain the SOC level. In [4], [5], the SOC information is combined with the area control error (ACE) signal to form the input for the BESS, so that the power command corrects the system frequency as well as the BESS SOC. In [6], a model predictive controller is utilized to manipulate the BESS power output considering the future system frequency response. In [7], [8], the participation factor of the BESS is gradually decreasing with the saturation/depletion of the BESS. RESs are also used to compensate for the long term energy deviation as in [9].

2. Filtering and decomposition: As the fast fluctuating component of the regulation signal is a zero-energy service [10] and the BESS is capable of dealing with fast fluctuating signals, various kinds of decomposition techniques are used to eliminate the long term energy deviation signal from the frequency error. The BESSs are only responsible for short term fluctuations. The system uses BESSs in the most effective way. Meanwhile, the BESSs seldom suffer from energy constrains. In [11], [12], filters with different time constants are used to generate suitable control signals for BESSs. In [13], a model based decomposition method is used to separate the signal within the suitable bandwidth.

Additionally, electrical vehicles connected to the grid (V2G) are also regarded as an alternative regulation resource. The control scheme is highly similar to the ones summarized above, and further constrained by the users' driving and charging behaviors [14].

II. Current Regulation Market for BESSs

A. Regulation signal

In regulation market operations, BESSs can respond to the traditional regulation signal or the dynamic regulation signal in Fig. 1. The traditional regulation signal is derived from area control error (ACE) in (1), processed with a set of low-pass filters and PI controllers.

$$\begin{aligned} ACE &= (P_{tie} - P_{tie,sched}) + B_f(f - 50) \\ &= \Delta P_{tie} + B_f \Delta f \end{aligned} \tag{1}$$

where ΔP_{tie} is the tie-line power error out of the control area, equivalent to the difference between the real tie-line power P_{tie} and the scheduled value $P_{tie,sched}$; B_f is the frequency bias of the control area, which is an estimation of the system response characteristic in MW/Hz.

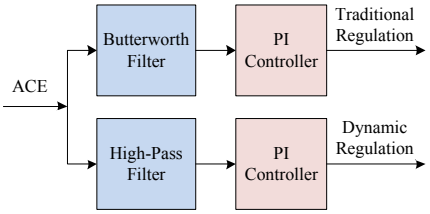

Fig. 1. Traditional and dynamic regulation signal generation.

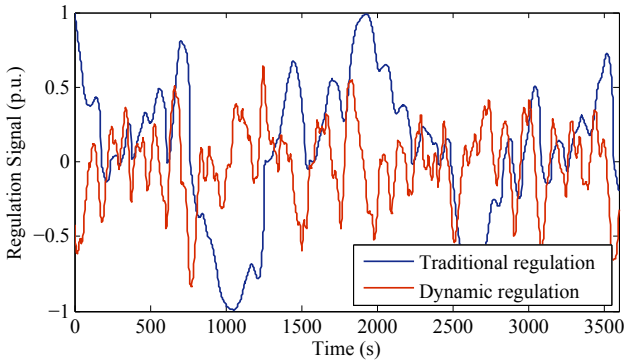

Fig. 2. Normalized traditional and dynamic regulation signals.

The dynamic regulation is also derived from the ACE through a high-pass filter and a PI controller to obtain the dynamic regulation signal. The dynamic regulation signal is distributed to very fast responding units, and these units will be rewarded with higher payments. In the United States, the fast regulation price triples the regular price [15]. Historical traditional and dynamic regulation signals for one hour is plotted in Fig. 2

B. Performance Evaluation Criteria

Since the system has its own inertia, frequency regulation units are not forced to respond strictly according to the commands. However, certain level of compliance is required. Energy market companies have their specific rules to calculate the performance of each unit. In this paper, the performance is evaluated using the PJM criteria [16].

The performance score consists of three performance scores considering three different aspects:

- Precision score (S_P)
- Delay score (S_D)
- Correlation score (S_C)

The scores are evaluated every one hour and the signal measurements are taken on a 10-second basis.

The precision score S_P in (2) measures the average errors between the unit command and its response.

$$S_P = 1 - \frac{1}{n}\sum_{t=1}^{n}\left|\frac{y(t)-u(t)}{\overline{u}_h}\right| \tag{2}$$

where $y(t)$ is the actual unit response; $u(t)$ is the regulation signal; and $\overline{u}_h$ is the hourly average value of the regulation signal.

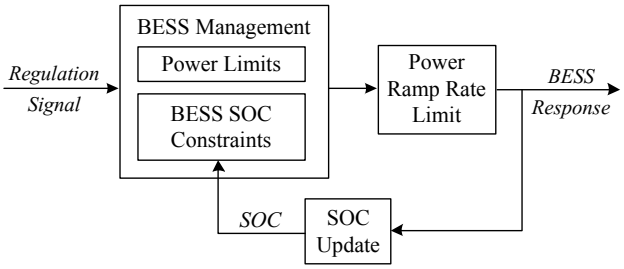

Fig. 3. A general BESS model for response testing.

The correlation score S_C measures the maximum correlation between the 50-minute regulation signal and the unit response with t seconds shifting (σ_t) in (3).

$$S_C = max(\sigma_0, \sigma_1, ..., \sigma_t) \qquad \forall t \in [0, 5\ min] \tag{3}$$

The delay score S_D is calculated from the time when the maximum correlation happens (t_σ) in (4).

$$S_D = \left|\frac{t_\sigma - 5\,min}{5\,min}\right| \tag{4}$$

The final score S in (5) is a weighted average of S_P, S_C and S_D:

$$S = A \cdot S_P + B \cdot S_C + C \cdot S_D \tag{5}$$

where parameters A, B, and C are decided by the market governor. In most cases, their values are equal, i.e. $A = B = C = 1/3$.

III. Regulation Simulations Studies

A. BESS modeling

A general BESS model is developed as plotted in Fig. 3, to simulate the real time response to regulation signals. The regulation signal will be processed by a rule-based BESS management system [17] constraining the power and SOC within the limits shown in (6) and (7):

Power limits:

$$P_E^{c,max} \le P(t) \le P_E^{d,max} \tag{6}$$

SOC limits:

$$SOC_{min} \le SOC(t) \le SOC_{max} \tag{7}$$

where $P_E^{d,max}$ is the maximum discharge rate; and $P_E^{c,max}$ is the maximum charge rate.

If $P(t)$ exceeds/falls below the power limits, the response power will be set as $P_E^{d,max}$ or $P_E^{c,max}$. If the state of charge $SOC(t)$ is greater than or equal to 0.8, the BESS cannot be charged anymore. If $SOC(t)$ is less than or equal to 0.2, the BESS cannot be discharged anymore.

The BESS response is further limited by the ramp rate. The chemical reactions in the battery can react within milliseconds. Therefore the power converters operation limit is the main ramp rate limiter in a BESS.

A SOC update block is also used to simulate the SOC value as the feedback to the BESS management system. The SOC

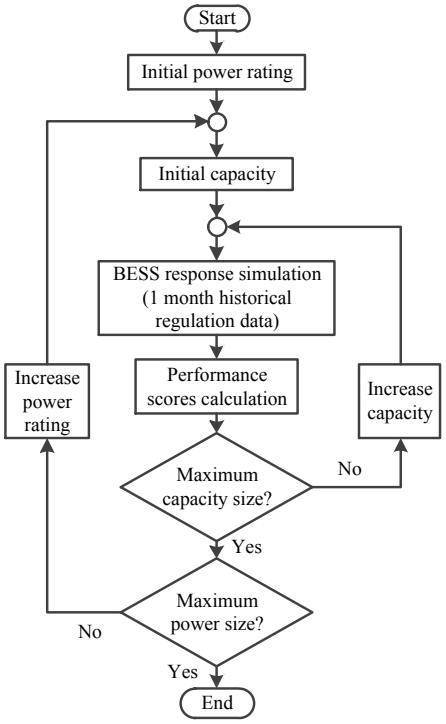

Fig. 4. Work flow for performance score simulations.

calculation is based on the simple coulomb counting method in (8):

$$SOC(t+1) = SOC(t) - \frac{P(t) \cdot \Delta t}{E_{BESS}} \tag{8}$$

where E_{BESS} is the rated BESS capacity; and Δt is the duration time of each interval.

B. Simulated performance scores

Performance score simulations are conducted using the BESS model and the historical real time operation regulation signal available at the PJM website [18]. The simulation procedure is described in Fig. 4. The simulations are conducted for different power ratings and capacity ratings. Given the same power rating, performance scores for each capacity setting is calculated according to (2) to (5).

The average scores and the respective score distribution ranges are plotted in Fig. 5. With the increase of the its energy capacity, the distribution range gets smaller. This means that the probability for the BESS to saturate or deplete is less, and thus the risk of getting a low score decreases. Besides, the averages are mostly located in the higher score ranges rather than in the middle of the ranges. Normally BESS will perform very well in a high-score range, and the chances to get low scores are comparatively rare. However, after the energy capacity increases further above 80 kWh, the average performance scores stay on the same level. In other words, for a BESS with a 20 kW power rating, 80 kWh energy capacity is totally sufficient for the highest score possible for regulation market participation.

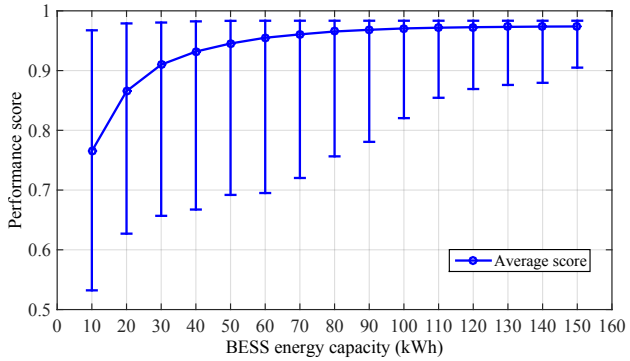

Fig. 5. Performance score simulations of different capacities, power rating = 100 kW.

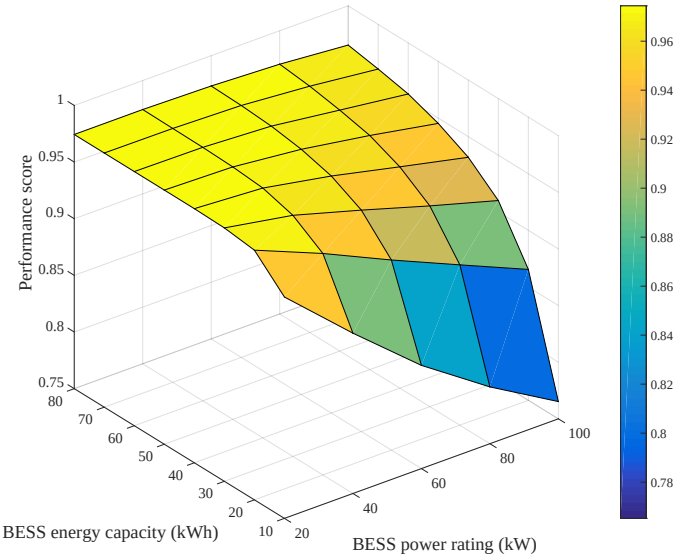

Fig. 6. Average scores with different power and energy settings.

Average performance scores with different energy capacity ratings as well as power ratings are presented in Fig. 6. With the increase of the power rating, a larger portion of regulation signal will be assigned to the BESS, demanding more energy to follow the commands. Therefore, given the same energy capacity and an increasing power rating, the performance deteriorates. While given the same power rating, the performance score increases with the increase in energy capacity, as plotted in Fig. 5.

According to the score surface, given x kW power rating, the energy capacity needs to be at least $0.5x$ to achieve a decent performance around 0.94 (orange color in Fig. 6). After $0.5x$, the surface becomes almost horizontal, meaning that the growth of the performance score is trivial.

Although it seems beneficial to increase the capacity since the score is highly related to the final revenue from the regulation market, capacity expansion cost is also high. Risk assessment needs to be done to decide the BESS capacity to be purchased.

TABLE I
BATTERIES CHARACTERISTICS [19]

	Vanadium	Lead-acid	Lithium-ion
Specific energy (Wh/kg)	20-25	30-50	110-160
Efficiency	70-88%	70-80%	80-90%
Life-cycle (80% capacity)	10,000-16,000	200-1,000	400-1,200
Operating temperature (°C)	10 to 45	-10 to 40	5 to 45

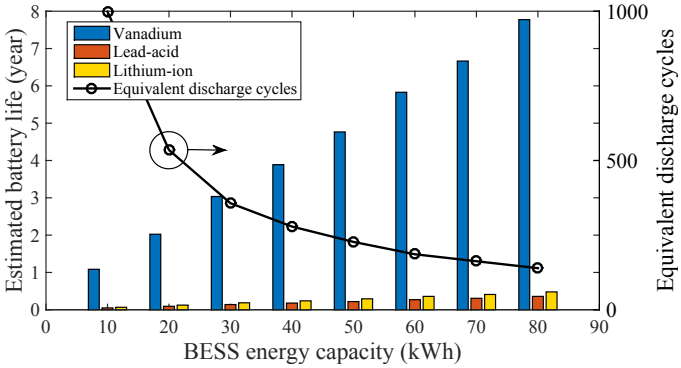

Fig. 7. Monthly equivalent discharge cycles and the estimated battery life time.

C. BESS lifetime estimation

Withe the BESS responses simulated in Section III.B, the BESS lifetime can be estimated. Since the lifetime model requires detailed battery testing results and fitting procedure, the equivalent discharge cycles are used instead to estimate the battery life as in (9) and (10).

$$Cycles = \sum_{t} P_{dis}(t)/E_{BESS} \tag{9}$$

$$Life(years) = \frac{Total\ Life\ Cycles}{Cycles\ per\ Year} \tag{10}$$

Three major batteries are compared in this paper: Vanadium, Lead-acid, and Lithium-ion. Their characteristics are summarized in Table I. Assume that the life-cycles for the three batteries are the average of the ranges given (13,000 for Vanadium, 600 for Lead-acid, and 800 for Lithium-ion), and the equivalent discharge cycles and the estimated battery lives are plotted in Fig. 7. When the capacity increases, the equivalent discharge cycles decreases nearly linearly. As a result, the lifetime increases. Vanadium batteries are notably more durable than the other two types. This is also the major advantage of vanadium batteries [19]. However, Vanadium batteries have a low specific energy, and will be heavy and bulky with a large capacity.

IV. COST-EFFECTIVENESS STUDIES

In this section, the BESSs capital investments, regulation revenue, and the cost-performance indexes are calculated based on real system data.

TABLE II
UNIT PRICES FOR DIFFERENT BATTERIES

	Cost		Power rating
	$/kW	$/kWh	
Vanadium	600 (∼1500)	100 (∼1000)	10 kW-3 MW
Lead-acid	300 (∼600)	200 (∼400)	0-20 MW
Lithium-ion	1200 (∼4000)	600 (∼2500)	0-100 kW

*US dollar as the monetary unit

TABLE III
NOTATIONS IN SECTION IV

Acronyms and Symbols	Description
CRF	Capital recovery factor
AC	Annualized capital investment ($/year)
TC	Total capital investment ($)
C_{kW}	Per unit power cost of BESS ($/kW)
C_{kWh}	Per unit energy cost of BESS ($/kWh)
R_P R_C	Power and capacity rewards for regulation ($)
REG_{PCP}	Regulation performance clearing price ($/MWh)
REG_{CCP}	Regulation capacity clearing price ($/MWh)

A. Equivalent annual cost

The capital investment of BESSs involves two parts: energy component ($/kWh) and power component ($/kW). General pricing information from the literature [19], [20], [21] is summarized in Table II. The total investment and the annualized cost are both calculated according to (11) to (13). Operation and maintenance cost for the three types of batteries are similar, therefore not considered in the calculation. Notations used are explained in Table III.

$$CRF(i,n) = \frac{i\cdot(1+i)^n}{(1+i)^n - 1} \tag{11}$$

$$AC = TC \cdot CRF(i,n) \tag{12}$$

where

$$TC = C_{kW}\cdot P_{BESS} + C_{kWh}\cdot E_{BESS} \tag{13}$$

According to the total cost values in Fig. 8, the Vanadium and Lead-acid batteries are much less expensive than the

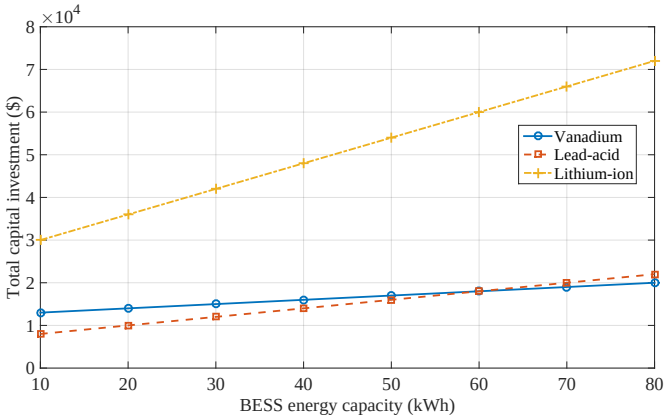

Fig. 8. Total capital investment for three batteries when power rating = 20 kW.

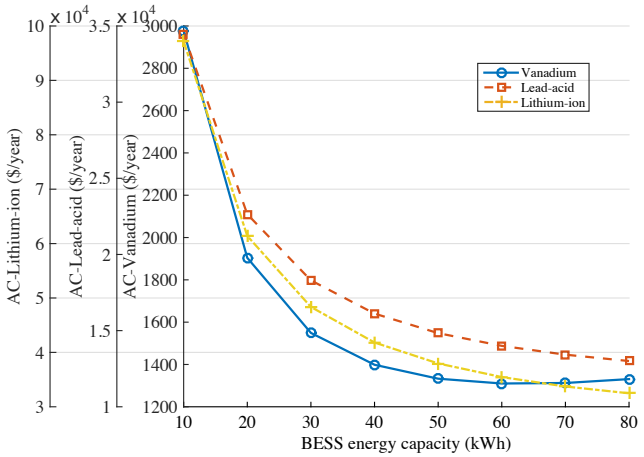

(a) AC for different energy capacity, power rating = 20 kW.

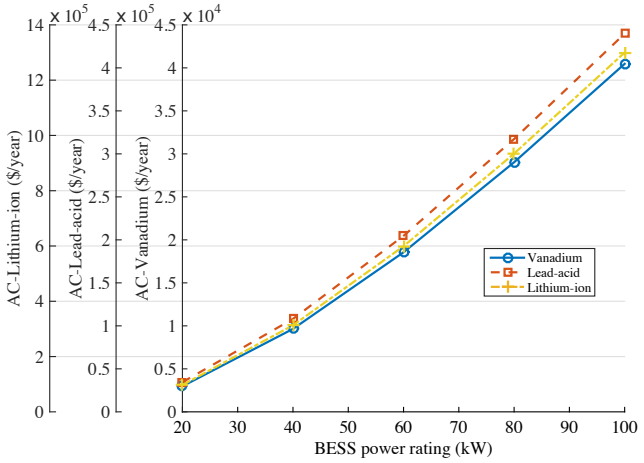

(b) AC for different power ratings, energy capacity = 10 kWh.

Fig. 9. Annualized capital investment for three batteries with different power and energy ratings.

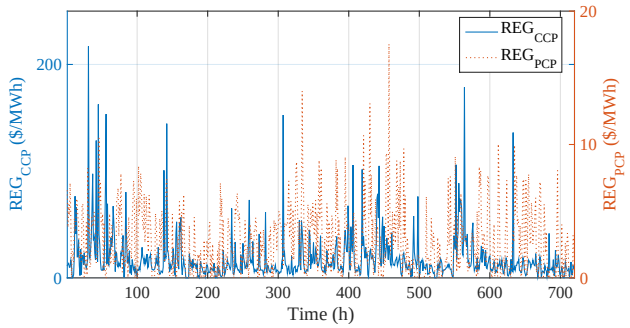

Fig. 10. Regulation price data for one month.

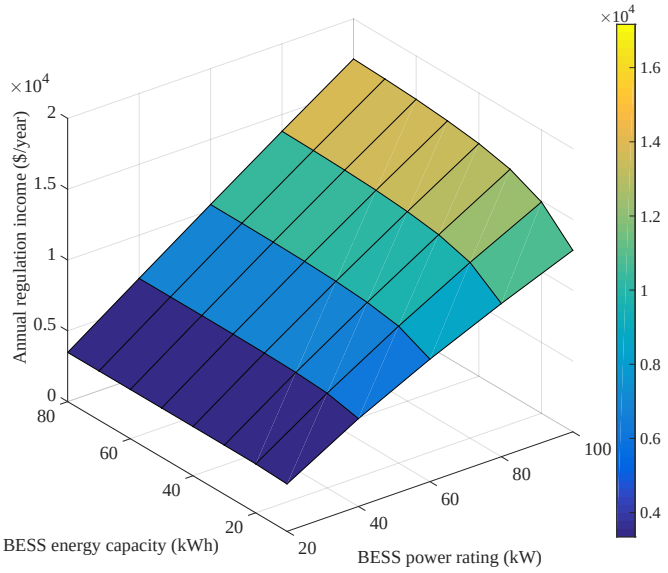

Fig. 11. Annualized regulation revenue for BESS power rating = 20 kW.

Lithium-ion battery. And the growth rates of the total cost for Vanadium and Lead-acid are lower, which means it is cheaper to expand their energy capacity. For Vanadium batteries, once the power rating is set, it is very convenient to expand the capacity by simply adding more volumes of electrolyte.

The annualized costs are plotted in Fig. 9(a). In Fig. 9(a), the annualized cost decreases resulting from the longer life cycles and decremental rate of expansion cost. Conversely, in Fig. 9(b), when the power rating increases, the regulation service requires more equivalent discharge cycles. Therefore, the annualized cost increases because of shorter battery life and the increase in the capital investment.

B. Regulation revenue

According to PJM rules and other power market rules, the regulation revenue consists of two parts: 1. the capacity revenue R_C in (14) for reserving the capacity, multiplies the hourly performance score; 2. the real performance revenue R_P in (15) considering real BESS movement mileage multiplies the score. Real hourly pricing data is plotted in Fig. 10.

$$R_C = P_{BESS} \cdot REG_{CCP} \cdot S \tag{14}$$

$$R_P = P_{BESS} \cdot Mileage\,Ratio \cdot REG_{PCP} \cdot S \tag{15}$$

The estimated total annual regulation revenue is plotted in Fig. 11. Generally speaking, devoting more power rating into the regulation market results in more revenue, although the regulation prices are fluctuating with time. Additionally, if the energy capacity if small, the rate of increase will be smaller, since the regulation revenue is also constrained by the performance score.

C. Cost-effectiveness studies

Given the estimated annual regulation revenue and the respective annualized cost, the cost-performance indexes are calculated based on the definition in (16). The CPI indicates how much income will be earned given the investment spent.

$$CPI = \frac{R_C + R_P}{AC} \tag{16}$$

The CPI values for different power and capacity settings are presented in Fig. 12. Overall, the Vanadium battery CPI

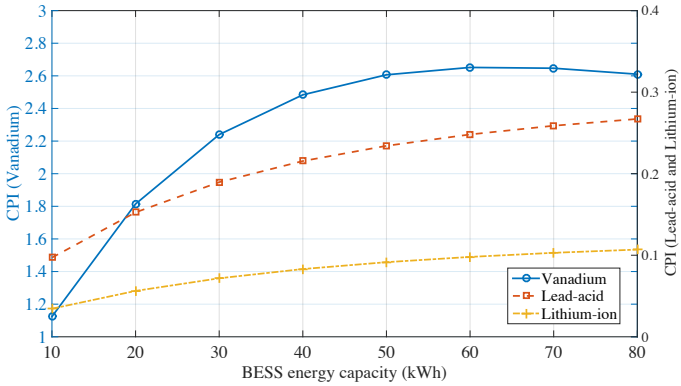

(a) Varying capacity settings, rated power = 20 kW.

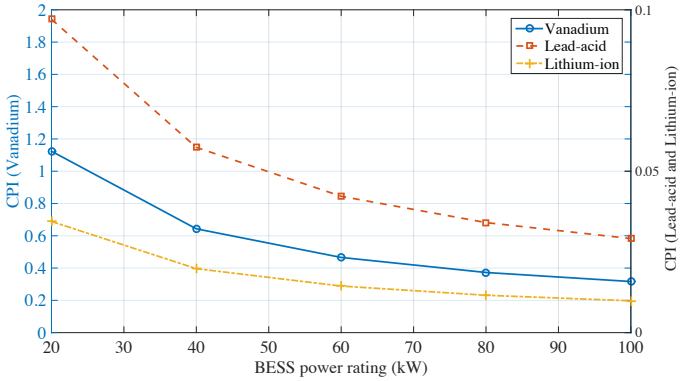

(b) Varying power ratings, rated capacity = 10 kWh.

Fig. 12. CPI with different BESS capacity and power settings.

is larger than 1 for most of the cases, and thus can earn more than the investment by simply participating in the regulation market. While for the Lead-acid and Lithium-ion, simply taking part in the regulation market cannot cover the investment cost.

In Fig. 12(a), it is cost-effective to increase the energy capacity rating. CPI increases with the capacity expansion, which is in accordance with income increase in Fig.11 and the AC drop in Fig. 9(a). While in Fig. 12(b), the power rating increase is not effective in earning more revenue. Even though the income increases according to Fig. 11, the high unit power price has a larger impact on the overall CPI, leading to the decreasing CPI.

V. Conclusions

In this paper, the BESS performance, capital investment, and regulation revenue are studied based on real system regulation signals and pricing, using a simplified BESS model.

For a BESS with a certain power rating, the performance score will increase with the capacity increase. However the increase is very limited when the capacity value exceeds 0.5 times the power rating value. Considering that capacity expansion is expensive, it is not cost effective to increase power rating, and the BESS power rating and capacity rating values should be under 1:2 to reach a high performance level without unnecessary expenditure.

References

[1] T. Sasaki, T. Kadoya, and K. Enomoto, "Study on load frequency control using redox flow batteries," *IEEE Trans. Power Syst.*, vol. 19, no. 1, pp. 660–667, Feb 2004.

[2] P. Mercier, R. Cherkaoui, and A. Oudalov, "Optimizing a battery energy storage system for frequency control application in an isolated power system," *IEEE Trans. Power Syst.*, vol. 24, no. 3, pp. 1469–1477, Aug 2009.

[3] A. Oudalov, D. Chartouni, and C. Ohler, "Optimizing a battery energy storage system for primary frequency control," *IEEE Trans. Power Syst.*, vol. 22, no. 3, pp. 1259–1266, Aug 2007.

[4] F. D. Mohammadi, M. J. Ghorbani, A. Feliachi, and M. A. Choudhry, "Novel load frequency control approach based on virtual area error in a microgrid including pv and battery," in *PES General Meeting — Conference Exposition, 2014 IEEE*, July 2014, pp. 1–5.

[5] Y. Cheng, M. Tabrizi, M. Sahni, A. Povedano, and D. Nichols, "Dynamic available agc based approach for enhancing utility scale energy storage performance," *IEEE Trans. Smart Grid*, vol. 5, no. 2, pp. 1070–1078, March 2014.

[6] M. Khalid and A. V. Savkin, "Model predictive control based efficient operation of battery energy storage system for primary frequency control," in *Control Automation Robotics Vision (ICARCV), 2010 11th International Conference on*, Dec 2010, pp. 2248–2252.

[7] X. Li, D. Hui, and X. Lai, "Battery energy storage station (bess)-based smoothing control of photovoltaic (pv) and wind power generation fluctuations," *IEEE Trans. Sustain. Energy*, vol. 4, no. 2, pp. 464–473, April 2013.

[8] I. Serban, R. Teodorescu, and C. Marinescu, "Energy storage systems impact on the short-term frequency stability of distributed autonomous microgrids, an analysis using aggregate models," *IET Renewable Power Generation*, vol. 7, no. 5, pp. 531–539, Sept 2013.

[9] J. Dang, J. Seuss, L. Suneja, and R. G. Harley, "Soc feedback control for wind and ess hybrid power system frequency regulation," *IEEE Journal of Emerging and Selected Topics in Power Electronics*, vol. 2, no. 1, pp. 79–86, March 2014.

[10] R. D. Masiello, B. Roberts, and T. Sloan, "Business models for deploying and operating energy storage and risk mitigation aspects," *Proceedings of the IEEE*, vol. 102, no. 7, pp. 1052–1064, July 2014.

[11] H. Amano, Y. Ohshiro, T. Kawakami, and T. Inoue, "Utilization of battery energy storage system for load frequency control toward large-scale renewable energy penetration," in *Innovative Smart Grid Technologies (ISGT Europe), 2012 3rd IEEE PES International Conference and Exhibition on*, Oct 2012, pp. 1–7.

[12] T. Masuta and A. Yokoyama, "Supplementary load frequency control by use of a number of both electric vehicles and heat pump water heaters," *IEEE Trans. Smart Grid*, vol. 3, no. 3, pp. 1253–1262, Sept 2012.

[13] C. A. Baone and C. L. DeMarco, "From each according to its ability: Distributed grid regulation with bandwidth and saturation limits in wind generation and battery storage," *IEEE Trans. Control Syst. Technol.*, vol. 21, no. 2, pp. 384–394, March 2013.

[14] F. Kennel, D. Gorges, and S. Liu, "Energy management for smart grids with electric vehicles based on hierarchical mpc," *IEEE Trans. Ind. Informat.*, vol. 9, no. 3, pp. 1528–1537, Aug 2013.

[15] (2013) Faster Frequency Regulation Triples in PJM. [Online]. Available: http://www.greentechmedia.com/articles/read/faster-frequency-regulation-triples-in-pjm

[16] (2009) PJM Manual 12: Balancing Operations. [Online]. Available: www.pjm.com

[17] S. X. Chen, T. Zhang, H. B. Gooi, R. D. Maciello, and W. Katzenstein, "Penetration rate and effectiveness studies of aggregated bess for frequency regulation," *approved for publication IEEE Trans. Smart Grid*, 2015.

[18] (2014) PJM Ancillary Services. [Online]. Available: http://www.pjm.com/markets-and-operations/ancillary-services.aspx

[19] C. Blanc, "Modeling of a vanadium redox flow battery electricity storage system," Ph.D. dissertation, Ecole Polytechnique Fédérale de Lausanne, 2009.

[20] H. Chen, T. N. Cong, W. Yang, C. Tan, Y. Li, and Y. Ding, "Progress in electrical energy storage system: A critical review," *Progress in Natural Science*, vol. 19, no. 3, pp. 291 – 312, 2009. [Online]. Available: http://www.sciencedirect.com/science/article/pii/S100200710800381X

[21] C. Menictas, M. Skyllas-Kazcos, and T. M. Lim, Eds., *Advances in Batteries for Medium and Large-Scale Energy Storage*. Woodhead Publishing, December 2014.